THE JOURNAL OF BIOLOGICAL CHEMISTRY VOL. 287, NO. 52, pp. 43876–43883, December 21, 2012

Localization and Substrate Selectivity of Sea Urchin Multidrug (MDR) Efflux Transporters*[S]

Received for publication, October 2, 2012, and in revised form, October 31, 2012 Published, JBC Papers in Press, November 2, 2012, DOI 10.1074/jbc.M112.424879

Tufan Gökirmak[‡], Joseph P. Campanale[‡], Lauren E. Shipp[‡], Gary W. Moy[‡], Houchao Tao[§], and Amro Hamdoun[‡1]

From the [‡]Marine Biology Research Division, Scripps Institution of Oceanography, University of California San Diego, La Jolla, California 92093 and the [§]Department of Molecular Biology, The Scripps Research Institute, La Jolla, California 92037

Background: MDR transporters are important for many human diseases, but their phylogenetic origins and diversity are poorly understood.
Results: Sea urchin MDR transporters homologous to ABCB1, ABCC1, and ABCG2 were characterized.
Conclusion: Substitutions in TMH6 tune substrate selectivity of ABCB1 in sea urchins.
Significance: Polyspecific MDR transport is conserved despite fine-tuning of substrate selectivity in different clades.

In this study, we cloned, expressed and functionally characterized *Stronglycentrotus purpuratus* (*Sp*) ATP-binding cassette (ABC) transporters. This screen identified three multidrug resistance (MDR) transporters with functional homology to the major types of MDR transporters found in humans. When overexpressed in embryos, the apical transporters *Sp*-ABCB1a, ABCB4a, and ABCG2a can account for as much as 87% of the observed efflux activity, providing a robust assay for their substrate selectivity. Using this assay, we found that sea urchin MDR transporters export canonical MDR susbtrates such as calcein-AM, bodipy-verapamil, bodipy-vinblastine, and mitoxantrone. In addition, we characterized the impact of nonconservative substitutions in the primary sequences of drug binding domains of sea urchin *versus* murine ABCB1 by mutation of *Sp*-ABCB1a and treatment of embryos with stereoisomeric cyclic peptide inhibitors (QZ59 compounds). The results indicated that two substitutions in transmembrane helix 6 reverse stereoselectivity of *Sp*-ABCB1a for QZ59 enantiomers compared with mouse ABCB1a. This suggests that subtle changes in the primary sequence of transporter drug binding domains could fine-tune substrate specificity through evolution.

Multidrug resistance (MDR)[2] transporters are membrane proteins that protect cells by efflux of xenobiotics and control cell function by efflux of morphogens and signaling molecules. These transporters are members of the ATP-binding cassette (ABC) transporter superfamily and include ABCB1, ABCC1, ABCC2, and ABCG2 (a.k.a., P-gp, MRP1, MRP2, and BCRP). Their substrates range from xenobiotics to endogenous peptides and lipids (1, 2), all of which can be transported out of cells against steep concentration gradients.

Despite the significance of these proteins in development and disease (3, 4), relatively little is known about their phylogenetic origins or functional diversity. Although MDR-like activity and homologous transporters have been described in several model organisms including worms (5), flies (6, 7), fishes (8, 9), molluscs (10), and sea urchins (11, 12), the similarity of these transporters to human homologs is unclear.

Whereas complementation studies suggest that broad substrate selectivity is conserved over large evolutionary distances (13–15), phylogenetic analyses indicate that there could be relatively little one-to-one orthology, with independent evolution of MDR-like transporters, each with potentially separate functions, in different classes of organisms (16, 17).

In this study we identified sea urchin homologs of the major types of MDR transporters and characterized their putative localizations and efflux activities. Despite having diverged from a common ancestor to humans >540 million years ago (18), most of the sea urchin MDR transporters exhibit similar localizations and efflux activities to the closest human homologs. However, by comparison of sea urchin and mouse ABCB1, we identified changes in the primary structure of their drug binding domains that could tune substrate selectivity. These results have implications for understanding the molecular basis of substrate recognition and evolution of MDR transporters.

EXPERIMENTAL PROCEDURES

Animals and Reagents—Purple sea urchins (*Strongylocentrotus purpuratus*) were collected and maintained in aquaria according to Campanale and Hamdoun (4). Calcein-AM (CAM) was purchased from Biotium (Hayward, CA). bodipy-verapamil (b-VER) and bodipy-vinblastine (b-VIN) were obtained from Invitrogen. Mitoxantrone (MX) was purchased from Sigma. QZ59-RRR and QZ59-SSS cyclic hexapeptides were synthesized according to Tao *et al.* (19). All stock solutions were prepared in dimethyl sulfoxide and diluted to the

* This work was supported, in whole or in part, by National Institutes of Health Grant HD058070 (to A. H.). This work was also supported by Krinsk Research Advancement Initiative (to A. H.).
[S] This article contains supplemental Methods and additional references, Figs. S1–S4, and Table S1.
[1] To whom correspondence should be addressed: Scripps Institution of Oceanography, University of California San Diego, 9500 Gilman Dr., 0202, La Jolla, CA, 92093. Tel.: 858-822-4303; Fax: 858-534-7313; E-mail: hamdoun@ucsd.edu.
[2] The abbreviations used are: MDR, multidrug resistance; ABC, ATP-binding cassette; b-VER, bodipy-verapamil; b-VIN, bodipy-vinblastine; CAM, calcein-AM; FP, fluorescent protein; HPF, hours postfertilization; LCK, lymphocyte-specific protein tyrosine kinase; MSD, membrane spanning domain; MX, mitoxantrone; NBD, nucleotide binding domain; P-gp, P-glycoprotein; Sp, *Stronglycoentrotus purpuratus*; TMH, transmembrane helix; Mm, *Mus musculus*.

TABLE 1
Summary of expressions, localizations and efflux activities of sea urchin ABC transporters
+++, high level protein expression; ++, medium level protein expression; +, low level protein expression.

Gene (GenBank ID)	Tag position	Expression level	Localization	Efflux activity				Addgene ID
				CAM	b-VIN	b-VER	MX	
Sp-ABCB1a (JQ390048)	C-mCherry	+	Apical	Yes				
	N-mCherry	+++	Apical	Yes	Yes	Yes		34939
	N-Cerulean	++	Apical				No	34944
	No tag	++		Yes				38036
Sp- ABCB4a (JQ354983)	C-mCherry	+	Apical	Yes				
	N-mCherry	+++	Apical	Yes	Yes	Yes		34941
	N-Cerulean	++	Apical				No	34945
Sp- ABCC1 (JQ354984)	C-mCherry	++	Basolateral	No				40587
	N-mCherry	+	Small apical vesicles	No				34942
Sp-ABCC5a (JQ354989)	C-mCherry	+	Basolateral	No				
	N-mCherry	++	Basolateral	No				35207
Sp-ABCC9a (JQ355003)	C-mCherry	+	Large apical vesicles	No				35208
	N-mCherry	++	Toxic, retained in ER[a]					
Sp- ABCG2a (JQ355004)	C-mCherry	+++	Apical	No	No	No		34943
	N-mCherry	++	Apical	No	No	No		
	C-Cerulean	+++	Apical				Yes	34946

[a] ER, endoplasmic reticulum.

final concentrations in filtered seawater. The final dimethyl sulfoxide concentration in the assays did not exceed 0.5%.

Cloning of Sea Urchin Transporters and Generation of cDNA Constructs—Sea urchin homologs of ABC transporter sequences were identified from the *S. purpuratus* genome V3.1. The full-length cDNA sequences of transporters were determined by 5′- and 3′-rapid amplification of cDNA ends (Clontech). Homology of the annotated sequences was verified by protein BLAST against the human sequence database in NCBI. All transporters were PCR-amplified with Phusion high fidelity DNA polymerase (New England Biolabs) using gene-specific primers. Transporters were cloned into pCS2+ (20) or variants of this vector (pCS2+8) that we developed for systematic screening of these large genes (Table 1 and supplemental Table S1).

Murinized sea urchin ABCB1a (L380F, F384I) was generated by site-directed mutagenesis and cloned into pCS2+8NmCherry. pCS-memb-mCherry, a general membrane mCherry marker fused to the membrane signal of lymphocyte-specific protein tyrosine kinase (LCK) and pCS-H2B-mRFP, containing histone H2B, a nuclear marker, were gifts from Dr. Scott Fraser (California Institute of Technology) and Dr. Sean Megason (Harvard University). Additional information on the constructs generated in this study (Table 1) is available through Addgene.

In Vitro Synthesis and Microinjection of ABC Transporter mRNA—Each DNA construct was linearized with NotI-HF (New England Biolabs) and used as template for *in vitro* transcription using the Sp6 Message Machine kit (Ambion, Austin, TX). Dejellied eggs were immobilized on protamine sulfate-coated coverslip dishes (Bioptechs, Butler, PA) and microinjected as described by Cheers and Ettensohn (21). For the localization and efflux assays, transporter mRNAs were injected at 1 μg/μl in ribonuclease-free ultrapure water. Some embryos on each dish were left without injection, to serve as controls for efflux activity assays. After injection, embryos were incubated at 14–15 °C for ~16 h until they reached early blastula.

Expression and Localization of Recombinant Sea Urchin ABC Transporters—N- and C-terminal mCherry fusions of ABC transporters were imaged in the epithelial cells of blastulae at 16 h postfertilization (HPF) on a Zeiss LSM 700 laser scanning confocal microscope (Jena) using a 20×, 0.8 NA, apochromatic air objective. Images were captured with the ZEN software package (Zeiss, revision 5.5) and prepared with ImageJ (National Institutes of Health) and Volocity (PerkinElmer Life Sciences).

Transporter Efflux Activity Assays—Efflux assays were performed as described previously (4). Briefly, efflux activity of each sea urchin ABC transporter was determined at ~16 HPF in embryos expressing recombinant ABC transporters, and controls. The microinjected and noninjected control embryos were incubated with CAM, b-VIN, b-VER, and MX in a final concentration of 250 nM, 125 nM, 125 nM, and 5 μM, at 15 °C for 90 min. Immediately before imaging, embryos incubated with b-VIN and b-VER were washed 10 times with filtered seawater to remove background fluorescence.

Intracellular fluorescence was measured from 4.1-μm-thick equatorial confocal sections of embryos. Images from 15–21 embryos from three separate experiments were collected for each transporter-drug pair; *i.e.* 5–7 embryos from each of 3 different batches.

The relative efflux activity of each transporter was determined by measuring the intracellular substrate fluorescence intensity per pixel in microinjected embryos relative to noninjected control embryos using the measurement module of Volocity.

Inhibition of Sp-ABCB1a and Sp-ABCB4a by QZ59 Enantiomers—Inhibition of *Sp*-ABCB1a, ABCB4a, and ABCB1a (L380F, F384I)-mediated CAM efflux by QZ59 enantiomers was determined in ~16 HPF embryos. The microinjected embryos expressing mCherry-tagged transporters and no-tag ABCB1a were incubated with CAM (250 nM) and QZ59-RRR (10 μm) or QZ59-SSS (10 μM) at 15 °C for 90 min. Intracellular calcein accumulation in embryos was measured as described above.

Statistics—Significant differences in substrate accumulation were evaluated by one-way ANOVA (JMP-9, SAS Institute Inc., Cary, NC). Post hoc multiple comparisons between injected mRNAs for each ABC-transporter were made using a Steel-

Dwass nonparametric test at a significance threshold of $p < 0.05$.

RESULTS

In this study, we cloned and characterized sea urchin homologs of six ABC transporters, including four putative MDR transporter homologs, *Sp*-ABCB1a, ABCB4a, ABCC1, and ABCG2a (Table 1). Sea urchins do not have ABCC2 or ABCC3 orthologs, but have a large expansion of C5 and C9 clades (22); therefore, we also examined representative members of each of these families.

First, we characterized the predicted membrane topologies (supplemental Fig. S1 and supplemental Methods). *Sp*-ABCB1a and *Sp*-ABCB4a (supplemental Fig. S1, *A* and *B*) have two membrane spanning domains (MSD), each consisting of six transmembrane helices (TMH), and two nuclear binding domains (NBD). *Sp*-ABCC1 and *Sp*-ABCC9a had the expected "long MRP" architectures with three MSDs and two NBDs (supplemental Fig. S1, *C* and *E*). *Sp*-ABCC5a had a "short MRP" topology with two MSDs (MSD_1 and MSD_2) and two NBDs (supplemental Fig. S1*D*). Finally, *Sp*-ABCG2a had one N-terminal NBD and one MSD (supplemental Fig. S1*F*). Collectively, the predicted topologies of the sea urchin ABC transporters were identical to those of mammalian homologs (23).

Expression and Localization of Sea Urchin ABC Transporters—To determine the subcellular location of these transporters, we generated and expressed mCherry fusions of each protein (Table 1 and Fig. 1). Because previous studies suggested that the position of the fluorescent protein (FP) tag may influence the behavior of transporters (24, 25), we examined the effect of tag position by expressing both N- and C-terminal fusions of each transporter. As expected, expression levels and localizations of transporters depended on tag position (Fig. 1 and Table 1).

For *Sp*-ABCB1a and ABCB4a both N- and C-terminal fusions localized to the apical membranes of polarized epithelial cells, but the N-terminal proteins accumulated to higher levels. *Sp*-ABCG2a fusions were also apically localized but exhibited the opposite pattern of expression, with the C-fusion expressing more robustly than the N-fusion (Fig. 1 and Table 1).

In general, ABCC proteins exhibited more significant variation with tag position. For example, the C-terminal fusion of *Sp*-ABCC1 localized to basolateral membranes, whereas the N-terminal fusion primarily localized to apical vesicles (Fig. 1 and Table 1). For *Sp*-ABCC5a, both N- and C-terminal fusions localized to basolateral membranes, but the N-terminal fusion expressed at higher levels than the C-terminal fusion (Fig. 1 and Table 1). Finally, C-terminal *Sp*-ABCC9a expressed strongly in large apical vesicles, whereas expression of the N-terminal fusion caused cellular toxicity and had cytoplasmic localization consistent with retention of the protein in endoplasmic reticulum (Fig. 1 and supplemental Fig. S2).

Identification of MDR-like Transporters Using Efflux Assays—Next, to determine whether these proteins had MDR-like efflux activity, we first screened each mCherry transporter fusion against fluorescent MDR transporter substrates. Based on a preliminary activity screen (Table 1) and the localization data, we selected N-terminal fusions of *Sp*-ABCB1a, ABCB4a, and ABCC5a and C-terminal fusions of *Sp*-ABCC1, ABCC9a, and ABCG2a for further analyses.

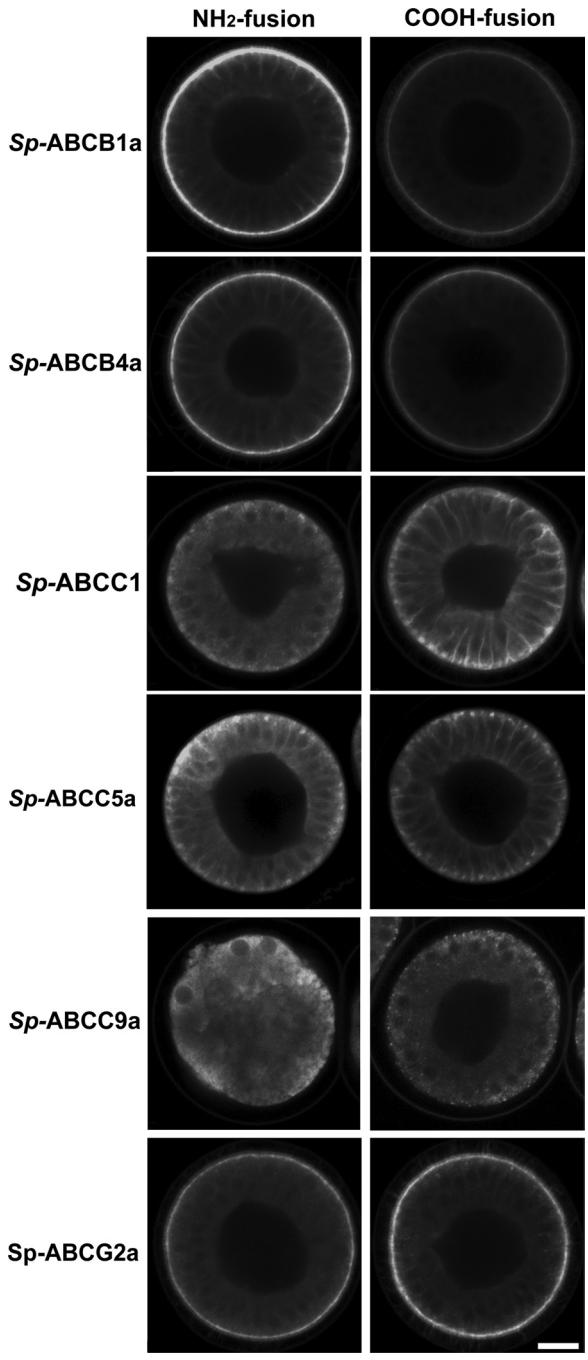

FIGURE 1. **Fluorescent protein tag position influences the expression of sea urchin ABC transporters in blastulae.** Both N- and C-terminal mCherry fusions of *Sp*-ABCB1a, ABCB4a, and ABCG2 localize to apical membranes. C-terminal *Sp*-ABCC1 and N-terminal and C-terminal fusions of *Sp*-ABCC5a localize to basolateral membranes. C-terminal fusion of *Sp*-ABCC9a localizes to apical vesicles. *Scale bar*, 20 μm.

The first substrate examined in detail was CAM, a nonfluorescent substrate for mammalian ABCB and ABCC-type MDR transporters. CAM is hydrolyzed by intracellular esterases to calcein, a fluorescent impermeable compound (26). Thus, in this assay, transporter activity reduces intracellular calcein fluorescence.

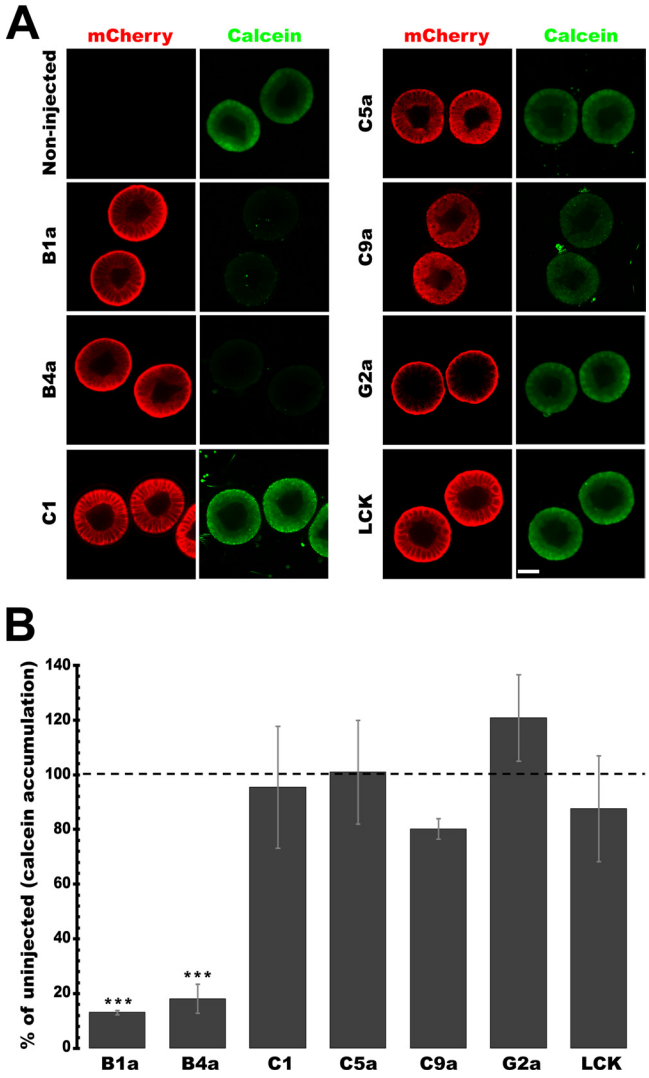

FIGURE 2. **Recombinant sea urchin ABC transporters have CAM efflux activity.** *A*, micrographs showing that overexpression of mCherry-tagged *Sp*-ABCB1a and ABCB4a reduces intracellular calcein accumulation significantly. *Sp*-ABCC1, ABCC5a, ABCC9, and ABCG2a, and LCK control have no effect on CAM accumulation. *Scale bar*, 35 μm. *B*, quantitative analysis of intracellular calcein accumulation in embryos expressing ABC transporters and LCK. ***, $p < 0.0001$ indicates the transporters significantly different from LCK. *Error bars*, S.D. $n = 18–20$ embryos from three separate experiments.

Expression of mCherry-tagged *Sp*-ABCB1a and ABCB4a significantly reduced intracellular calcein accumulation (Fig. 2*A*). In contrast, *Sp*-ABCC1, ABCC5a, ABCC9a, and ABCG2a did not reduce calcein accumulation (Fig. 2*A*). Intracellular calcein accumulation in *Sp*-ABCB1a- and ABCB4a-expressing embryos was significantly lower than LCK control (***, $p <$ 0.0001). For these two proteins accumulation was reduced to 13.21% (±0.77) and 18.24% (±5.24) of noninjected control embryos (Fig. 2*B*).

Although *Sp*-ABCG2a also localized to the apical membrane, it did not significantly alter calcein accumulation, with *Sp*-ABCG2a expressing embryos accumulating 120.8% (±15.86) of noninjected controls. This, along with the observation that the LCK fusions also do not significantly alter calcein accumulation, indicated that the assay specifically measured efflux activity rather than passive alterations of membrane permeability.

Characterization of MDR Transporters Using Fluorescent Drugs—To further characterize the substrate selectivity of the sea urchin MDR homologs, we tested efflux activities of the apical transporters identified above against the fluorescent drugs and drug analogs, b-VIN, b-VER, and MX, which are substrates of mammalian MDR transporters (27–29).

Sp-ABCB1a and ABCB4a reduced intracellular accumulation of b-VIN and b-VER whereas *Sp*-ABCG2a had no effect on their accumulation (Fig. 3*A*). Intracellular b-VIN accumulation in embryos expressing mCherry-tagged *Sp*-ABCB1a, ABCB4a, and ABCG2a were 26.73% (±6.32), 21.09% (±4.23), and 117.04% (±11) of the noninjected control embryos, respectively (Fig. 3*B*). For b-VER, the respective ratios were 10.54% (±3.84), 8.4% (±2.45), and 109.26% (±21.3).

Because mammalian ABCG2 is a MX transporter, we investigated efflux activities of *Sp*-ABCB1a, ABCB4a, and ABCG2a for this compound. Mitoxantrone is red fluorescent, and thus we constructed cyan fluorescent protein fusions of *Sp*-ABCB1a and ABCB4a, ABCG2a (Table 1) to allow us to simultaneously confirm activity and expression in these assays. Whereas intracellular accumulation of mitoxantrone was significantly reduced by *Sp*-ABCG2a, it was unaffected by *Sp*-ABCB1a and ABCB4a (Fig. 3*A*). Intracellular MX accumulation in embryos expressing *Sp*-ABCB1a, ABCB4a, and ABCG2 was 103.29% (± 10.62), 102.31% (±13.49), and 69.37% (±9.6) of noninjected control embryos, respectively (Fig. 3*B*).

Analysis of Stereoselectivity of Sp-ABCB1a and ABCB4a Using QZ59-RRR and QZ59-SSS—The results above largely indicated conservation of substrate selectivity between sea urchin and human MDR transporters. However, given the lack of one-to-one orthology of these proteins (16, 17) and the obvious variation in primary structure of their drug binding domains, we next sought to determine whether there could be fine-scale changes in substrate selectivity of sea urchin MDR transporters compared with their mammalian homologs.

We focused on *Sp*-ABCB1a and ABCB4a because they are homologous to mouse ABCB1a, for which a high resolution structure has recently been determined (30). In addition, the murine ABCB1a structure was characterized bound to stereoisomeric cyclic peptide inhibitors (QZ59-RRR and QZ59-SSS), and the residues that interact with these compounds were identified. Because of differences in these interactions, the cyclic peptide QZ59-SSS (IC_{50} = 2.7 ± 0.25 μM) is a more potent inhibitor of mouse ABCB1a-mediated calcein efflux than QZ59-RRR (IC_{50} = 8.5 ± 0.47 μM) (30).

To determine whether similar residues were present in sea urchins, we aligned *Sp*-ABCB1a and ABCB4a proteins with mouse ABCB1a (Fig. 4*A*) focusing on TMH 6 and 12, which are critical for QZ59 binding (30). In *Sp*-ABCB1a, there are four nonconservative substitutions in these helices (Fig. 4*A*): F332L, I336F, M982F, and S989G (Leu-380, Phe-384, Phe-1036 and Gly-1043 in *Sp*-ABCB1a). In contrast, *Sp*-ABCB4a has mouse-like residues at Phe-332 and Ile-336 (Phe-360 and Ile-364 in *Sp*-ABCB4a) in TMH6 and unique residues, M982I and S989A (Ile-1005 and Ala-1012 in *Sp*-ABCB4a), in TMH12 (Fig. 4*A*).

Based on this observation, we hypothesized that *Sp*-ABCB1a and ABCB4a would have differences in QZ59 stereoisomer selectivity compared with one another and with mouse. Con-

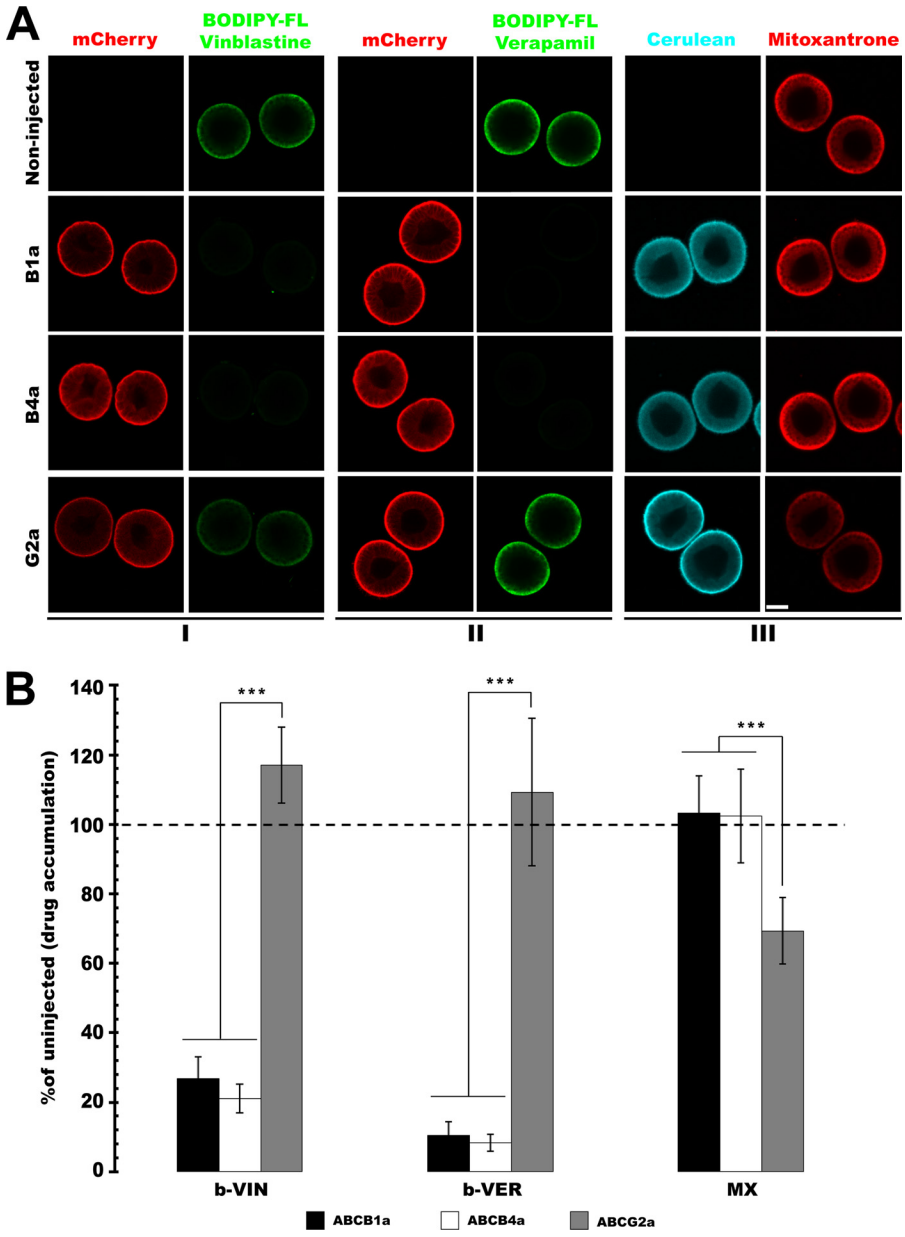

FIGURE 3. **Sea urchin MDR proteins transport similar substrates to their mammalian homologs.** *A*, micrographs showing that overexpression of *Sp*-ABCB1a and ABCB4a, but not ABCG2a, reduces intracellular b-VIN (*I*) and b-VER (*II*) accumulation significantly (***, $p < 0.0001$). Overexpression of cerulean (*CFP*)-tagged *Sp*-ABCG2a, but not ABCB1a or ABCB4, reduces intracellular MX (*III*) accumulation significantly (*, $p < 0.01$). *Scale bar*, 35 μm. *B*, quantitative analysis of intracellular b-VIN, b-VER, and MX accumulation in embryos expressing apical MDR transporters. $n = 14–18$ embryos from three separate experiments. *Error bars*, S.D.

sistent with this hypothesis QZ59-RRR was 2.14 times more effective at inhibition of *Sp*-ABCB1a-mediated CAM efflux than QZ59-SSS (Fig. 4*C*). The mCherry tag did not mediate these differences because *Sp*-ABCB1a lacking the tag showed a similar pattern of selectivity (supplemental Fig. S3). In contrast, QZ59-RRR and QZ59-SSS inhibited 7.34% (±2.32) and 40.21% (±4.87) of *Sp*-ABCB4a mediated CAM efflux, respectively, a pattern of stereoselectivity similar to that of mouse ABCB1a (Fig. 4*B*). This indicated that two unique nonconservative substitutions in TMH6 of *Sp*-ABCB1a, Leu-380 and Phe-384, may be responsible for the reversal of QZ59 selectivity.

To investigate the role of Leu-380 and Phe-384 in reversal of QZ59 selectivity of *Sp*-ABCB1a, we substituted these residues with corresponding mouse residues (L380F, F384I) and tested inhibition of the CAM efflux by the QZ59 enantiomers (Fig. 4*A*). Murinization of TMH6 residues caused reversal of stereoselectivity of *Sp*-ABCB1a similar to mouse ABCB1a and *Sp*-ABCB4a by reducing the level of QZ59-RRR-mediated CAM efflux inhibition significantly, but did not change the potency of QZ59-SSS (Fig. 4*B*). These results indicate that nonconservative substitutions in the primary structure of TMH6 could be important for tuning their substrate selectivity.

DISCUSSION

In this study, we exploited the expression of recombinant transporters in sea urchin embryos to determine the function and subcellular location of sea urchin ABC transporters. We identified three transporters, *Sp*-ABCB1a, ABCB4a, and

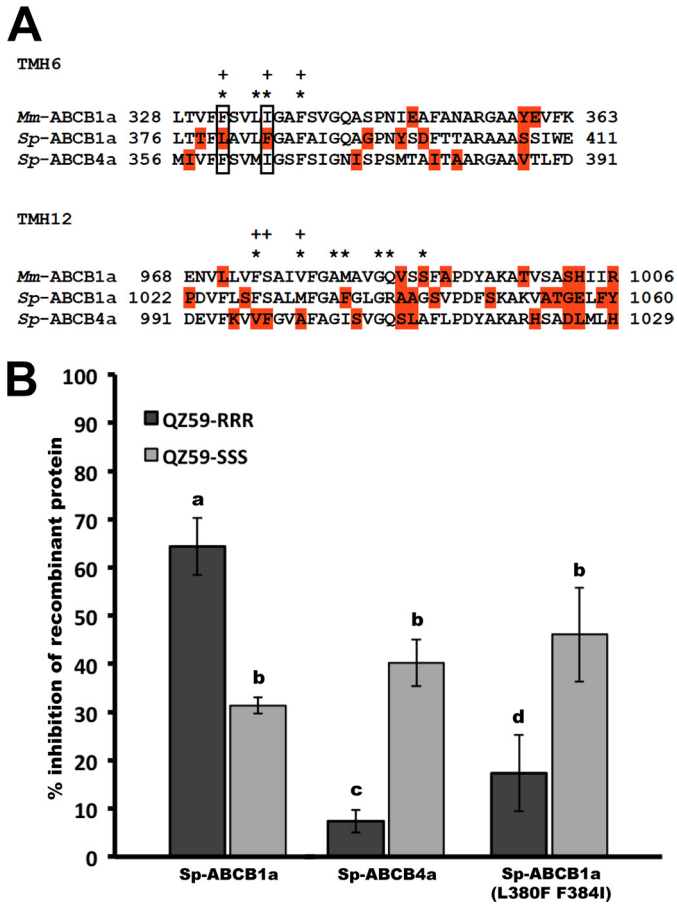

FIGURE 4. **Differences in inhibition of sea urchin *Sp*-ABCB1a- and ABCB4a-mediated CAM efflux by QZ59 enantiomers.** *A*, protein alignments of TMH6 and 12 of sea urchin *Sp*-ABCB1a and ABCB4a with mouse *Mm*-ABCB1a showing that Leu-380 and Phe-384 residues are unique nonconservative substitutions in *Sp*-ABCB1a drug binding domain. Residues in close proximity with QZ59-RRR (+) and QZ59-SSS (*) (30). Residues marked in *red* are nonconservative substitutions. *B*, quantitative analysis of the inhibition of intracellular calcein accumulation by QZ59 stereoisomers (10 μM) in embryos expressing mCherry-tagged *Sp*-ABCB1a, ABCB4, and ABCB1a (L380F, F384I) fusions. *Bars* with *different letters* are significantly different from each other ($p \leq 0.002$). $n = 18–20$ embryos from three separate experiments. *Error bars*, S.D.

ABCG2, with clear apical localization and MDR-like activities. Expression of these proteins caused dramatic increases in efflux of canonical fluorescent substrates, such as calcein-AM, bodipy-vinblastine, bodipy-verapamil, and mitoxantrone. Notably, as much as 87% of the observed activity in embryos came from the recombinant transporter, providing a robust assay for transporter function.

Among the ABCCs, *Sp*-ABCC1 and ABCC5a localized to basolateral membranes, as do their human homologs (31, 32). One interesting observation was the localization of *Sp*-ABCC9a to large apical vesicles (Fig. 3 and supplemental Fig. S4), which is similar in morphology to those seen with localization of a closely related mammalian protein, ABCC8 (SUR1), in large vesicles of islet cells (33). Considering that ABCC8 (SUR1) and ABCC9 (SUR2) are closely related and that the sea urchin lacks an ABCC8 gene in its genome, it is possible that *Sp*-ABCC9a may have a SUR1-like function in sea urchin embryos; particularly, because sea urchin embryos express both ABCC9 (34) and insulin-like molecules (35) in early development.

In this study, we tested whether the fluorescent protein fusion could alter localization or function of the transporters. Several observations suggest that the locations and activities for the fluorescent protein-tagged MDRs were relevant. First, we found that all of the apically expressed mCherry fusions (*Sp*-ABCB1a, ABCB4a, and ABCG2) had robust and specific efflux activities (Figs. 2 and 3). Second, for *Sp*-ABCB1a, the apical localization of the fusion is in agreement with a recent study indicating its apical localization with antibodies (17). Third, all of the proteins, including *Sp*-ABCC1, ABCC5a, and ABCC9a, had similar subcellular localizations to their closest mammalian homologs. Nonetheless, other approaches will be required to determine the endogenous transporter distribution within the embryo. For example, *in situ* hybridization revealed that *Sp*-ABCB1a mRNA is expressed ubiquitously in the embryo, whereas *Sp*-ABCC5a is restricted to a subset of cells (34).

The results of this study have implications for understanding the molecular basis of substrate recognition by MDR transporters. One of our findings was the general pattern of conservation of substrate selectivity, despite divergence of these proteins from a common ancestor by >540 million years (18). One explanation could be that although the primary sequences of many cellular defense proteins diverge, their tertiary structures remain conserved (36). Indeed, a recent crystal structure of P-glycoprotein (P-gp) from *Caenorhaditis elegans* indicates that the overall architecture of P-gp-type transporters is conserved (37).

Previous studies on P-gp demonstrated that although drug transporters are generally quite polyspecific, there are measurable differences in how closely related substrates bind to and inhibit these transporters. One example is handling of the cyclic hexapeptides QZ59-RRR and QZ59-SSS, where the SSS enantiomer is a more potent inhibitor of mouse P-gp-mediated CAM efflux than the RRR enantiomer (30). This is presumably because SSS occupies two distinct binding sites in the drug-binding pocket whereas QZ59-RRR occupies only one (30, 38, 39).

When comparing the potency of the same stereoisomer pair in sea urchin ABCB1a, we found the opposite relationship with QZ59-RRR being a more potent inhibitor than QZ59-SSS (Fig. 4). These results are consistent with our observation of two unique nonconservative changes in key residues of the amino acid sequences of *Sp*-ABCB1a TMH 6 (Fig. 4*A*), which contribute to QZ59 binding sites in mouse P-gp (30). Strikingly, murinization of these two residues reversed QZ59 inhibition of CAM efflux back to the mouse profile, suggesting that subtle changes in the primary structure of the drug binding domains can influence the substrate specificity of MDR transporters.

Another difference between sea urchin and mammalian ABC transporters is the lack of MX activity of sea urchin ABCB1a (Fig. 3). In mammals, MX is a substrate for both ABCG2 and ABCB1, although it is less effectively transported by the latter transporter (27). However, in sea urchin, only ABCG2a has MX efflux activity. One possibility is that the steric changes created by the aromatic substitutions, *versus* small hydrophobic residues, reduce MX efflux activity of *Sp*-ABCB1a.

In summary, this study was a step toward understanding the structural and functional evolution of MDR transporters in

deuterostomes, the branch of evolution leading to the vertebrates. This is important because, unlike other highly conserved protein families (40, 41), the frequency of one-to-one orthology in ABC transporters is low (16, 17). It is conceivable that MDR transporter homologs in different organisms evolved independently, each adapted for different substrates in each organism. Further confounding the situation is the contradictory observation from complementation studies suggesting that substrate selectivity is conserved over large evolutionary spans (13–15).

As alluded to previously, many of the changes in sequences of these proteins may simply act to conserve their tertiary structure, and thus their general substrate selectivity (37). Here we observed that subtle changes in the primary structure of these proteins could tune their function without destroying the broader pattern of substrate selectivity. This tuning could have considerable adaptive implications, as is seen in polymorphism of other key cellular defenses (42, 43). In each of these cases, modest changes in primary structure have dramatic implications for the ability of the organism to adapt to its environment. Based on our results, we hypothesize that similar changes in drug binding pockets could be critical for evolution of the MDR transporters. As our study suggests, the structural and functional comparisons necessary to address this question are also informative for understanding the molecular basis of transporter substrate recognition.

Acknowledgments—We thank Drs. Scott Fraser and Sean Megason for membrane and nuclear marker constructs, Phillip Zerofski for collecting sea urchins, and Dr. Victor. D. Vacquier for helpful scientific discussions.

REFERENCES

1. Dean, M., Hamon, Y., and Chimini, G. (2001) The human ATP-binding cassette (ABC) transporter superfamily. *J. Lipid Res.* **42,** 1007–1017
2. Leslie, E. M., Deeley, R. G., and Cole, S. P. (2005) Multidrug resistance proteins: role of P-glycoprotein, MRP1, MRP2, and BCRP (ABCG2) in tissue defense. *Toxicol. Appl. Pharmacol.* **204,** 216–237
3. Gottesman, M. M., Fojo, T., and Bates, S. E. (2002) Multidrug resistance in cancer: role of ATP-dependent transporters. *Nat. Rev. Cancer* **2,** 48–58
4. Campanale, J. P., and Hamdoun, A. (2012) Programmed reduction of ABC transporter activity in sea urchin germline progenitors. *Development* **139,** 783–792
5. Broeks, A., Gerrard, B., Allikmets, R., Dean, M., and Plasterk, R. H. (1996) Homologues of the human multidrug resistance genes MRP and MDR contribute to heavy metal resistance in the soil nematode *Caenorhabditis elegans*. *EMBO J.* **15,** 6132–6143
6. Tarnay, J. N., Szeri, F., Iliás, A., Annilo, T., Sung, C., Le Saux, O., Váradi, A., Dean, M., Boyd, C. D., and Robinow, S. (2004) The dMRP/CG6214 gene of *Drosophila* is evolutionarily and functionally related to the human multidrug resistance-associated protein family. *Insect Mol. Biol.* **13,** 539–548
7. Vache, C., Camares, O., Cardoso-Ferreira, M. C., Dastugue, B., Creveaux, I., Vaury, C., and Bamdad, M. (2007) A potential genomic biomarker for the detection of polycyclic aromatic hydrocarbon pollutants: multidrug resistance gene 49 in *Drosophila melanogaster*. *Environ. Toxicol. Chem.* **26,** 1418–1424
8. Caminada, D., Zaja, R., Smital, T., and Fent, K. (2008) Human pharmaceuticals modulate P-gp1 (ABCB1) transport activity in the fish cell line PLHC-1. *Aquat. Toxicol.* **90,** 214–222
9. Zaja, R., Munić, V., Klobucar, R. S., Ambriović-Ristov, A., and Smital, T. (2008) Cloning and molecular characterization of apical efflux transporters (ABCB1, ABCB11 and ABCC2) in rainbow trout (*Oncorhynchus mykiss*) hepatocytes. *Aquat. Toxicol.* **90,** 322–332
10. Luckenbach, T., and Epel, D. (2008) ABCB- and ABCC-type transporters confer multixenobiotic resistance and form an environment-tissue barrier in bivalve gills. *Am. J. Physiol. Regul. Integr. Comp. Physiol.* **294,** R1919–1929
11. Hamdoun, A. M., Cherr, G. N., Roepke, T. A., and Epel, D. (2004) Activation of multidrug efflux transporter activity at fertilization in sea urchin embryos (*Strongylocentrotus purpuratus*). *Dev. Biol.* **276,** 452–462
12. Bosnjak, I., Uhlinger, K. R., Heim, W., Smital, T., Franekić-Colić, J., Coale, K., Epel, D., and Hamdoun, A. (2009) Multidrug efflux transporters limit accumulation of inorganic, but not organic, mercury in sea urchin embryos. *Environ. Sci. Technol.* **43,** 8374–8380
13. Raymond, M., Gros, P., Whiteway, M., and Thomas, D. Y. (1992) Functional complementation of yeast *ste6* by a mammalian multidrug resistance *mdr* gene. *Science* **256,** 232–234
14. Tommasini, R., Evers, R., Vogt, E., Mornet, C., Zaman, G. J., Schinkel, A. H., Borst, P., and Martinoia, E. (1996) The human multidrug resistance-associated protein functionally complements the yeast cadmium resistance factor 1. *Proc. Natl. Acad. Sci. U.S.A.* **93,** 6743–6748
15. van Veen, H. W., Callaghan, R., Soceneantu, L., Sardini, A., Konings, W. N., and Higgins, C. F. (1998) A bacterial antibiotic-resistance gene that complements the human multidrug-resistance P-glycoprotein gene. *Nature* **391,** 291–295
16. Sheps, J. A., Ralph, S., Zhao, Z., Baillie, D. L., and Ling, V. (2004) The ABC transporter gene family of *Caenorhabditis elegans* has implications for the evolutionary dynamics of multidrug resistance in eukaryotes. *Genome Biol.* **5,** R15
17. Whalen, K., Reitzel, A. M., and Hamdoun, A. (2012) Actin polymerization controls the activation of multidrug efflux at fertilization by translocation and fine-scale positioning of ABCB1 on microvilli. *Mol. Biol. Cell* **23,** 3663–3672
18. Sea Urchin Genome Sequencing Consortium, Sodergren, E., Weinstock, G. M., Davidson, E. H., Cameron, R. A., Gibbs, R. A., Angerer, R. C., Angerer, L. M., Arnone, M. I., Burgess, D. R., Burke, R. D., Coffman, J. A., Dean, M., Elphick, M. R., Ettensohn, C. A., Foltz, K. R., Hamdoun, A., Hynes, R. O., Klein, W. H., Marzluff, W., McClay, D. R., Morris, R. L., Mushegian, A., Rast, J. P., Smith, L. C., Thorndyke, M. C., Vacquier, V. D., Wessel, G. M., Wray, G., Zhang, L., Elsik, C. G., Ermolaeva, O., Hlavina, W., Hofmann, G., Kitts, P., Landrum, M. J., Mackey, A. J., Maglott, D., Panopoulou, G., Poustka, A. J., Pruitt, K., Sapojnikov, V., Song, X., Souvorov, A., Solovyev, V., Wei, Z., Whittaker, C. A., Worley, K., Durbin, K. J., Shen, Y., Fedrigo, O., Garfield, D., Haygood, R., Primus, A., Satija, R., Severson, T., Gonzalez-Garay, M. L., Jackson, A. R., Milosavljevic, A., Tong, M., Killian, C. E., Livingston, B. T., Wilt, F. H., Adams, N., Bellé, R., Carbonneau, S., Cheung, R., Cormier, P., Cosson, B., Croce, J., Fernandez-Guerra, A., Geneviève, A. M., Goel, M., Kelkar, H., Morales, J., Mulner-Lorillon, O., Robertson, A. J., Goldstone, J. V., Cole, B., Epel, D., Gold, B., Hahn, M. E., Howard-Ashby, M., Scally, M., Stegeman, J. J., Allgood, E. L., Cool, J., Judkins, K. M., McCafferty, S. S., Musante, A. M., Obar, R. A., Rawson, A. P., Rossetti, B. J., Gibbons, I. R., Hoffman, M. P., Leone, A., Istrail, S., Materna, S. C., Samanta, M. P., Stolc, V., Tongprasit, W., Tu, Q., Bergeron, K. F., Brandhorst, B. P., Whittle, J., Berney, K., Bottjer, D. J., Calestani, C., Peterson, K., Chow, E., Yuan, Q. A., Elhaik, E., Graur, D., Reese, J. T., Bosdet, I., Heesun, S., Marra, M. A., Schein, J., Anderson, M. K., Brockton, V., Buckley, K. M., Cohen, A. H., Fugmann, S. D., Hibino, T., Loza-Coll, M., Majeske, A. J., Messier, C., Nair, S. V., Pancer, Z., Terwilliger, D. P., Agca, C., Arboleda, E., Chen, N., Churcher, A. M., Hallböök, F., Humphrey, G. W., Idris, M. M., Kiyama, T., Liang, S., Mellott, D., Mu, X., Murray, G., Olinski, R. P., Raible, F., Rowe, M., Taylor, J. S., Tessmar-Raible, K., Wang, D., Wilson, K. H., Yaguchi, S., Gaasterland, T., Galindo, B. E., Gunaratne, H. J., Juliano, C., Kinukawa, M., Moy, G. W., Neill, A. T., Nomura, M., Raisch, M., Reade, A., Roux, M. M., Song, J. L., Su, Y. H., Townley, I. K., Voronina, E., Wong, J. L., Amore, G., Branno, M., Brown, E. R., Cavalieri, V., Duboc, V., Duloquin, L., Flytzanis, C., Gache, C., Lapraz, F., Lepage, T., Locascio, A., Martinez, P., Matassi, G., Matranga, V., Range, R., Rizzo, F., Röttinger, E., Beane, W., Bradham, C., Byrum, C., Glenn, T., Hussain, S., Manning, G., Miranda, E., Thomason, R., Walton, K., Wikramanayke, A., Wu, S. Y., Xu, R., Brown, C. T., Chen, L., Gray, R. F.,

Lee, P. Y., Nam, J., Oliveri, P., Smith, J., Muzny, D., Bell, S., Chacko, J., Cree, A., Curry, S., Davis, C., Dinh, H., Dugan-Rocha, S., Fowler, J., Gill, R., Hamilton, C., Hernandez, J., Hines, S., Hume, J., Jackson, L., Jolivet, A., Kovar, C., Lee, S., Lewis, L., Miner, G., Morgan, M., Nazareth, L. V., Okwuonu, G., Parker, D., Pu, L. L., Thorn, R., and Wright, R. (2006) The genome of the sea urchin Strongylocentrotus purpuratus. *Science* **314,** 941–952

19. Tao, H., Weng, Y., Zhuo, R., Chang, G., Urbatsch, I. L., and Zhang, Q. (2011) Design and synthesis of selenazole-containing peptides for cocrystallization with P-glycoprotein. *ChemBioChem* **12,** 868–873
20. Turner, D. L., and Weintraub, H. (1994) Expression of achaete-scute homolog 3 in Xenopus embryos converts ectodermal cells to a neural fate. *Genes Dev.* **8,** 1434–1447
21. Cheers, M. S., and Ettensohn, C. A. (2004) Rapid microinjection of fertilized eggs. *Methods Cell Biol.* **74,** 287–310
22. Goldstone, J. V., Hamdoun, A., Cole, B. J., Howard-Ashby, M., Nebert, D. W., Scally, M., Dean, M., Epel, D., Hahn, M. E., and Stegeman, J. J. (2006) The chemical defensome: environmental sensing and response genes in the *Strongylocentrotus purpuratus* genome. *Dev. Biol.* **300,** 366–384
23. Sharom, F. J. (2008) ABC multidrug transporters: structure, function and role in chemoresistance. *Pharmacogenomics* **9,** 105–127
24. Haggie, P. M., Stanton, B. A., and Verkman, A. S. (2004) Increased diffusional mobility of CFTR at the plasma membrane after deletion of its C-terminal PDZ binding motif. *J. Biol. Chem.* **279,** 5494–5500
25. Orbán, T. I., Seres, L., Ozvegy-Laczka, C., Elkind, N. B., Sarkadi, B., and Homolya, L. (2008) Combined localization and real-time functional studies using a GFP-tagged ABCG2 multidrug transporter. *Biochem. Biophys. Res. Commun.* **367,** 667–673
26. Essodaigui, M., Broxterman, H. J., and Garnier-Suillerot, A. (1998) Kinetic analysis of calcein and calcein-acetoxymethylester efflux mediated by the multidrug resistance protein and P-glycoprotein. *Biochemistry* **37,** 2243–2250
27. Litman, T., Brangi, M., Hudson, E., Fetsch, P., Abati, A., Ross, D. D., Miyake, K., Resau, J. H., and Bates, S. E. (2000) The multidrug-resistant phenotype associated with overexpression of the new ABC half-transporter, MXR (ABCG2). *J. Cell Sci.* **113,** 2011–2021
28. Crivellato, E., Candussio, L., Rosati, A. M., Bartoli-Klugmann, F., Mallardi, F., and Decorti, G. (2002) The fluorescent probe bodipy-FL-verapamil is a substrate for both P-glycoprotein and multidrug resistance-related protein (MRP)-1. *J. Histochem. Cytochem.* **50,** 731–734
29. Kimchi-Sarfaty, C., Gribar, J. J., and Gottesman, M. M. (2002) Functional characterization of coding polymorphisms in the human MDR1 gene using a vaccinia virus expression system. *Mol. Pharmacol.* **62,** 1–6
30. Aller, S. G., Yu, J., Ward, A., Weng, Y., Chittaboina, S., Zhuo, R., Harrell, P. M., Trinh, Y. T., Zhang, Q., Urbatsch, I. L., and Chang, G. (2009) Structure of P-glycoprotein reveals a molecular basis for poly-specific drug binding. *Science* **323,** 1718–1722
31. Nies, A. T., Jedlitschky, G., König, J., Herold-Mende, C., Steiner, H. H., Schmitt, H. P., and Keppler, D. (2004) Expression and immunolocalization of the multidrug resistance proteins, MRP1-MRP6 (ABCC1-ABCC6), in human brain. *Neuroscience* **129,** 349–360
32. Chen, Z. S., and Tiwari, A. K. (2011) Multidrug resistance proteins (MRPs/ABCCs) in cancer chemotherapy and genetic diseases. *FEBS J.* **278,** 3226–3245
33. Geng, X., Li, L., Watkins, S., Robbins, P. D., and Drain, P. (2003) The insulin secretory granule is the major site of K_{ATP} channels of the endocrine pancreas. *Diabetes* **52,** 767–776
34. Shipp, L. E., and Hamdoun, A. (2012) ATP-binding cassette (ABC) transporter expression and localization in sea urchin development. *Dev. Dyn.* **241,** 1111–1124
35. de Pablo, F., Chambers, S. A., and Ota, A. (1988) Insulin-related molecules and insulin effects in the sea urchin embryo. *Dev. Biol.* **130,** 304–310
36. Lepesheva, G. I., and Waterman, M. R. (2011) Structural basis for conservation in the CYP51 family. *Biochim. Biophys. Acta* **1814,** 88–93
37. Jin, M. S., Oldham, M. L., Zhang, Q., and Chen, J. (2012) Crystal structure of the multidrug transporter P-glycoprotein from Caenorhabditis elegans. *Nature* **490,** 566–569
38. Pajeva, I. K., Globisch, C., and Wiese, M. (2009) Comparison of the inward- and outward-open homology models and ligand binding of human P-glycoprotein. *FEBS J.* **276,** 7016–7026
39. Klepsch, F., and Ecker, G. F. (2010) Impact of the recent mouse P-glycoprotein structure for structure-based ligand design. *Mol. Inform.* **29,** 276–286
40. Chervitz, S. A., Aravind, L., Sherlock, G., Ball, C. A., Koonin, E. V., Dwight, S. S., Harris, M. A., Dolinski, K., Mohr, S., Smith, T., Weng, S., Cherry, J. M., and Botstein, D. (1998) Comparison of the complete protein sets of worm and yeast: orthology and divergence. *Science* **282,** 2022–2028
41. Croce, J. C., Wu, S. Y., Byrum, C., Xu, R., Duloquin, L., Wikramanayake, A. H., Gache, C., and McClay, D. R. (2006) A genome-wide survey of the evolutionarily conserved Wnt pathways in the sea urchin *Strongylocentrotus purpuratus*. *Dev. Biol.* **300,** 121–131
42. Wirgin, I., Roy, N. K., Loftus, M., Chambers, R. C., Franks, D. G., and Hahn, M. E. (2011) Mechanistic basis of resistance to PCBs in Atlantic tomcod from the Hudson River. *Science* **331,** 1322–1325
43. Prasad, K. V., Song, B. H., Olson-Manning, C., Anderson, J. T., Lee, C. R., Schranz, M. E., Windsor, A. J., Clauss, M. J., Manzaneda, A. J., Naqvi, I., Reichelt, M., Gershenzon, J., Rupasinghe, S. G., Schuler, M. A., and Mitchell-Olds, T. (2012) A gain-of-function polymorphism controlling complex traits and fitness in nature. *Science* **337,** 1081–1084